Using the apparent diffusion coefficient histogram analysis to predict response to neoadjuvant chemotherapy in patients with breast cancer: comparison among three region of interest selection methods

Xiaochuan Geng[#], Dandan Zhang[#], Shiteng Suo, Jie Chen, Fang Cheng, Kebei Zhang, Qing Zhang, Lan Li, Yang Lu, Jia Hua, Zhiguo Zhuang

Department of Radiology, Renji Hospital, Shanghai Jiao Tong University School of Medicine, Shanghai, China

Contributions: (I) Conception and design: X Geng, D Zhang; (II) Administrative support: J Hua, Z Zhuang; (III) Provision of study materials or patients: S Suo, X Geng; (IV) Collection and assembly of data: X Geng, D Zhang; (V) Data analysis and interpretation: X Geng, D Zhang; (VI) Manuscript writing: All authors; (VII) Final approval of manuscript: All authors.

[#]These authors contributed equally to this work.

Correspondence to: Zhiguo Zhuang; Jia Hua. No. 160 Pujian Rd., Shanghai 200127, China. Email: zhiguozhuang@163.com; jill_huajia@yeah.net.

Background: The apparent diffusion coefficient (ADC) value using histogram analysis is helpful to predict responses to neoadjuvant chemotherapy (NAC) in breast cancer. However, the measurement method has not reached a consensus. This study was to assess the diagnostic performance of the ADC histogram analysis at predicting patient response prior to NAC in breast cancer patients using different region of interest (ROI) selection methods.

Methods: A total of 75 patients who underwent diffusion weighted imaging (DWI) prior to NAC were retrospectively enrolled from February 2017 to December 2019. Images were measured using small 2-dimensional (2D) ROI, large 2D ROI, and volume ROI methods. The measurement time and ROI size were recorded. Histopathologic responses were acquired using the Miller-Payne grading system after surgery. The inter- and intra-observer repeatability was analyzed and the ADC histogram values from the three ROI methods were compared. The efficacy of each method at predicting patient response prior to NAC was assessed using the area under the receiver operating characteristic curve (AUC) for the whole study population and subgroups according to molecular subtype.

Results: Among the 75 enrolled patients, 26 (34.67%) were responsive to NAC therapy. The ADC histogram values were significantly different among the three ROI methods ($P \leq 0.038$). Inter- and intra-observer repeatability of the large 2D ROI method and the volume ROI method was generally greater than that observed with the 2D ROI method. The 10% ADC value of the large 2D ROI method showed the greatest AUC (0.701) in the whole study population and in the luminal subgroup (AUC 0.804). The volume ROI method required significantly more time than the other two ROI methods ($P<0.001$).

Conclusions: The small 2D ROI method is not appropriate for predicting response prior to NAC in breast cancer patients due to the poor repeatability. When choosing the ROI method and the histogram parameters for predicting response prior to NAC in breast cancer patients using ADC-derived histogram analysis, 10% of the large 2D ROI method is recommended, especially in luminal A subtype patients.

Keywords: Breast neoplasms; neoadjuvant therapy; diffusion magnetic resonance imaging; observer variation

Submitted Jan 27, 2022. Accepted for publication Mar 18, 2022.

doi: 10.21037/atm-22-1078

View this article at: https://dx.doi.org/10.21037/atm-22-1078

Introduction

Neoadjuvant chemotherapy (NAC) has been shown to increase the disease-free and overall survival rates in patients with operable breast cancer and represents an appropriate regimen for patients with locally advanced breast cancer (1,2). Predicting responsiveness to NAC may help to identify patients who will benefit from alternative therapeutic regimens.

Imaging plays an important role in predicting response to NAC in breast cancer. The imaging method include ultrasound, mammography, Magnetic resonance imaging (MRI), integrated positron emission tomography (PET) with computed tomography (CT) (PET/CT) and PET/MRI, etc. The biomarkers for response prediction derived from imaging include tumor size (diameter, area, volume), apparent diffusion coefficient (ADC) value, signal enhancement ratio (SER), standard uptake value (SUV), etc. ADC aims at reflecting the biological properties of breast cancer trough parameters extracted from quantitative diffusion weighted imaging (DWI) that may change earlier before the morphological changes are detectable, during NAC.

Although ADC value has been shown to be helpful in predicting a patient's responses to NAC (3,4), there are some inconsistencies (5-11). These conflicting results might be partly attributed to the absence of a standardize measurement method applied to obtain ADC value. Moreover, the conventionally used average ADC value cannot fully reflect tumor heterogeneity, which may result from cancer nests, ductal components, intratumoral necrosis, or fibrosis (12). Recently, a histogram analysis method has been introduced to investigate tumor heterogeneity (13).

The histogram method has been applied to predict the early response to NAC in patients with breast cancer and other types of malignancies (14-19). However, there is currently no consensus on the tumor region of interest (ROI) delineation method, some authors using volume ROIs method while others 2-dimensional (2D) ROIs (14,15,20,21). One study has applied histogram analysis to explore how ROIs can influence the measurement of the ADC value while predicting breast cancer response prior to NAC (22).

Therefore, this current study investigated the repeatability of three ROI methods; assessed the influence of different ROI methods on ADC-derived histogram values; and compared the clinical feasibility of different ROI methods using ADC-derived histogram analysis in predicting a response in breast cancer patients prior to administration of NAC. We present the following article in accordance with the STARD reporting checklist (available at https://atm.amegroups.com/article/view/10.21037/atm-22-1078/rc).

Methods

Patients

The study was conducted in accordance with the Declaration of Helsinki (as revised in 2013) and approved by institutional ethics board of Renji Hospital (No. KY2021-116-B). Informed consent was not required due to the retrospective nature of the study. A total of 106 patients, from Renji hospital clinical database between February 2017 and December 2019, were enrolled for this retrospective study. The inclusion criteria are displayed in *Figure 1*. The inclusion criterials were applied: (I) Histologically confirmed breast cancer by core needle biopsy before NAC; (II) MRI prior to NAC; (III) NAC prior to surgery; (IV) surgery after NAC; (V) lesions measurable on ADC map. The following patients (n=31) were excluded: (I) 19 patients (61%) with poor image quality; (II) 6 patients (19%) with software unrecognizable; (III) 1 male patient (3%); and (IV) 5 patients (16%) with tumors containing large necrotic or cystic compartments. Finally, 75 female patients were recruited, with a mean age of 50 years (range, 26–73 years). The basic clinical characteristics of the patients are summarized in *Table 1*.

Histopathological analysis

Patients who responded to NAC therapy were defined by the absence of any identifiable invasive malignant cell or strictly ductal carcinoma *in situ* after surgery, according to the Miller-Payne grading system (23). The status of the estrogen receptor (ER), progesterone receptor (PR), and human epidermal growth factor receptor 2 (HER2) were assessed by immunohistochemistry. The ER and PR status were expressed as percentages (%). In classifying the HER2 gene expression, negative status was determined using scores of 0 and 1+, while positive status was determined by a score of 3+. When the score was 2+, fluorescent in situ hybridization (FISH) was performed to verify HER2 status (FISH+ positive). Breast cancer molecular subtypes were classified into three subtypes including luminal type, HER2-enriched, and triple negative, as described in previous studies (22,24-26). Luminal type was defined as tumor cells with nuclear ER and/or PR staining >10%. Luminal type breast cancers include two subtypes, luminal A and B. Luminal A was defined as ER and/or PR staining >10% and HER2 negative. Luminal B was defined as ER and/or PR staining >10%

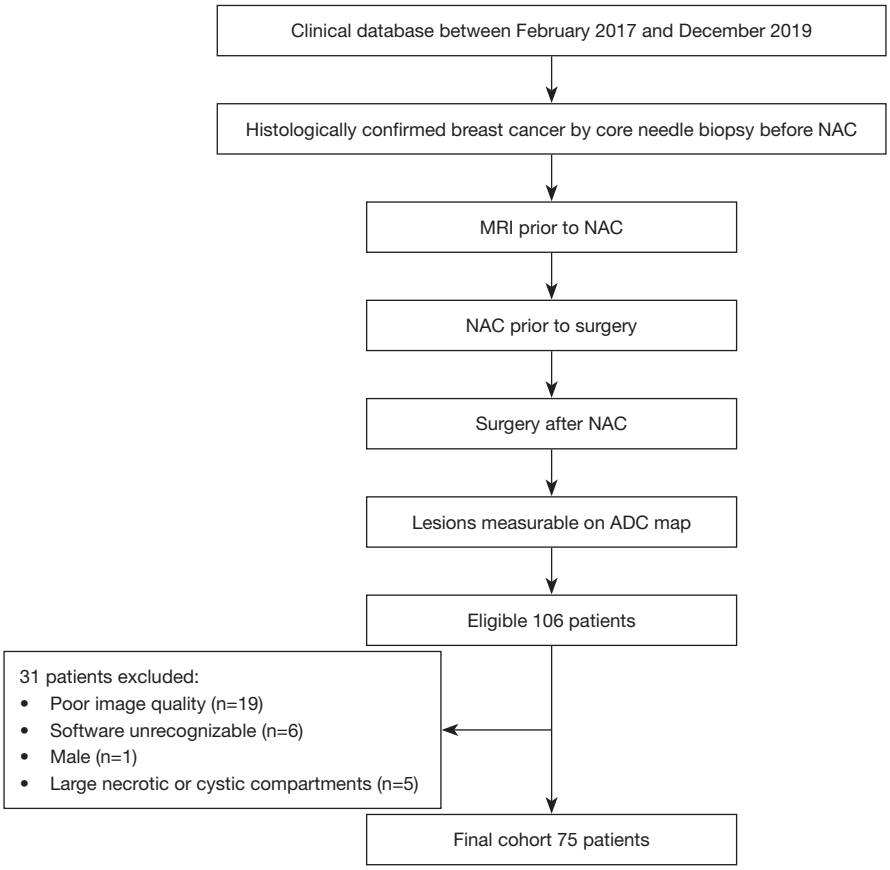

Figure 1 A flow chart of the study design depicting the number of patients. NAC, neoadjuvant chemotherapy; MRI, magnetic resonance imaging; ADC, apparent diffusion coefficient.

Table 1 Characteristics of the responders and non-responders before NAC

Characteristics	Responders (n=26)	Non-responders (n=49)	P
Age (years), mean ± SD	50±12	50±11	0.965
Menstruation			
Y	12	28	0.364
N	14	21	
ER expression (%)	18.35±32.14	52.39±36.78	<0.001*
PR expression (%)	27.35±29.30	36.98±32.19	0.208
HER2 expression			
Positive	18	21	0.030*
Negative	8	28	
Luminal A			
Y	5	25	0.007*
N	21	24	

Table 1 (*continued*)

Table 1 (*continued*)

Characteristics	Responders (n=26)	Non-responders (n=49)	P
Luminal B			
Y	14	20	0.281
N	12	29	
Luminal type			
Y	19	45	0.029*
N	7	4	
HER2 enriched			
Y	4	1	0.027*
N	22	48	
Triple negative			
Y	3	3	0.411
N	23	46	
TIC type			
I	5	13	0.580
II	16	22	
III	5	9	
Enhanced pattern			
Mass	22	30	0.053
Non-mass	4	19	
D (cm), mean ± SD	3.98±1.98	3.96±2.02	0.683
Size			
Small 2D ROI (cm^2), median (IQR)	0.15 (0.16)	0.16 (0.22)	0.684
Large 2D ROI (cm^2), median (IQR)	5.58 (5.09)	4.98 (6.63)	0.832
Volume ROI (cm^3), median (IQR)	12.39 (15.97)	11.08 (16.61)	0.920
Tumor type			
IC	11	18	
IDC	14	28	
ILC	0	3	
Others	1	0	

*, indicates statistical significance (P<0.05). NAC, neoadjuvant chemotherapy; SD, standard deviation; ER, estrogen receptor; PR, progesterone receptor; HER2, human epidermal growth factor receptor 2; TIC, time-intensity curve; D, maximum tumor diameter; 2D, 2-dimensional; ROI, region of interest; IQR, inter quartile range; IC, invasive carcinoma (which type of invasive carcinomas was not further classified); IDC, invasive ductal carcinoma; ILC, invasive lobular carcinoma; Y, yes; N, no.

and HER2 positive. HER2-enriched was defined as ER and PR staining <10% with HER2 positive. Triple negative was defined as ER and PR staining <10%, and HER2 negative.

Magnetic resonance imaging (MRI)

All patients underwent MRI using a 3.0 T MR scanner (Philips Medical Systems, Achieva, Best, The Netherlands)

in the prone position, using a four-channel breast array coil.

All MR images were acquired using the following sequences: an axial DWI sequence, a fat-suppressed T2-weighted sagittal sequence, and an axial T1-weighted sequence. Finally, an axial dynamic contrast-enhanced MRI (DCE-MRI) was performed with three-dimensional (3D) T1-weighted fast spoiled gradient-echo sequences before and after injection of a contrast agent (0.1 mmol/kg body weight Gd-DPTA, Bayer Healthcare, Magnevist, Germany). For DWI, images were acquired with a single shot spin-echo-planar sequence, using the following parameters: repetition time/echo time (TR/TE), 2,681/82 ms; field of view, 230×240 mm; matrix, 224×224; slice thickness, 3 mm; 40 slices with 0 mm gap; number of excitation (NEX), 3; b-values, 0 and 800 sec/mm^2.

Imaging analysis

Two breast radiologists (Xiaochuan Geng with 8 and Dandan Zhang with 2 years of experience in breast MRI) independently performed the ROI placements, which was repeated two months later. Both radiologists were blinded to the histological results and response to NAC. DWI image analysis was performed with MATLAB (MathWorks, version R2012b, Natick, Massachusetts, USA), and ADC maps were generated using a monoexponential model using the following formula:

$$ADC = \frac{\ln S_0 - \ln S_b}{b} \quad [1]$$

where S_0 and S_b represent DWI signal intensity at b=0 and 800 s/mm^2, respectively. Using lesion hyperintensity on high b-value DWI and DCE-MRI images as reference, ROIs were drawn manually on ADC maps using MATLAB. Necrosis, cystic, and hemorrhage sites were carefully avoided. Three ROI methods were applied (*Figure 2*). The small 2D ROI method was delineated in the area where the lowest intensity inside the lesion was visualized. The large 2D ROI method covered a single slice showing the largest area of the whole lesion. The volume ROI method covered the whole lesion on all slices, that were then combined to form a 3D-ROI. The histogram of the ADC values was then calculated using the MATLAB software for every method. The parameters derived from the histogram analysis included the mean; standard deviation (SD); minimum; maximum; 10% and 25%, median, 75%, and 90% percentiles; skewness; and kurtosis. Finally, measurement time was computed using tic and toc functions on MATLAB. Skewness was used to measure the asymmetry, and kurtosis was used to measure the peakedness of the distribution (26). The ROI size, enhanced pattern, TIC type, were also recorded.

Statistical analysis

Continuous variables were expressed as mean ± SD or median [interquartile range (IQR)] according to the distribution. Categorical variables were presented as a count. The inter- and intra-observer repeatability for the 3 ROI methods were analyzed using interclass correlation coefficient (ICC; 0.00–0.20 represents poor correlation; 0.21–0.40 indicates fair correlation; 0.41–0.60 indicates moderate correlation; 0.61–0.80 represents good correlation; and 0.81–1.00 represents excellent correlation). The histogram ADC parameters (mean, standard deviation, minimum, maximum, median, 10%, 25%, 75%, 90% of ADC values) of the responders versus the non-responders were compared using unpaired Student's *t*-tests for the 3 ROI methods. The differences in the histogram ADC parameters among the 3 ROI methods were compared using one-way analysis of variance (ANOVA). The measurement time was averaged and compared using paired-sample Student's *t*-tests. Receiver operating characteristic (ROC) curves were constructed to assess the ability of the 3 ROI methods to differentiate responders from non-responders. According to arbitrary guidelines, the accuracy of prediction was defined as less accurate (AUC: 0.5–0.7), moderately accurate (AUC: 0.7–0.9), highly accurate (AUC: 0.9–1). Comparisons between ROC curves were performed with the method used by DeLong *et al.* (27).

A P value less than 0.05 was considered statistically significant. Statistical analysis was performed using SPSS (IBM, version 21.0, Armonk, New York, USA), Medcalc (MedCalc Software Ltd., version 19.0.7, Ostend, Belgium) and EmpowerStats (2009 X&Y Solutions. Inc., IN, USA).

Results

Clinical characteristics

Table 1 presents the clinical characteristics of the patients. Out of the 75 patients, 26 (35%) showed a histopathologically confirmed response. Based on the immunohistochemistry results, there were significant differences in the ER and HER2 status between responders and non-responders (P<0.001 and P=0.030, respectively;

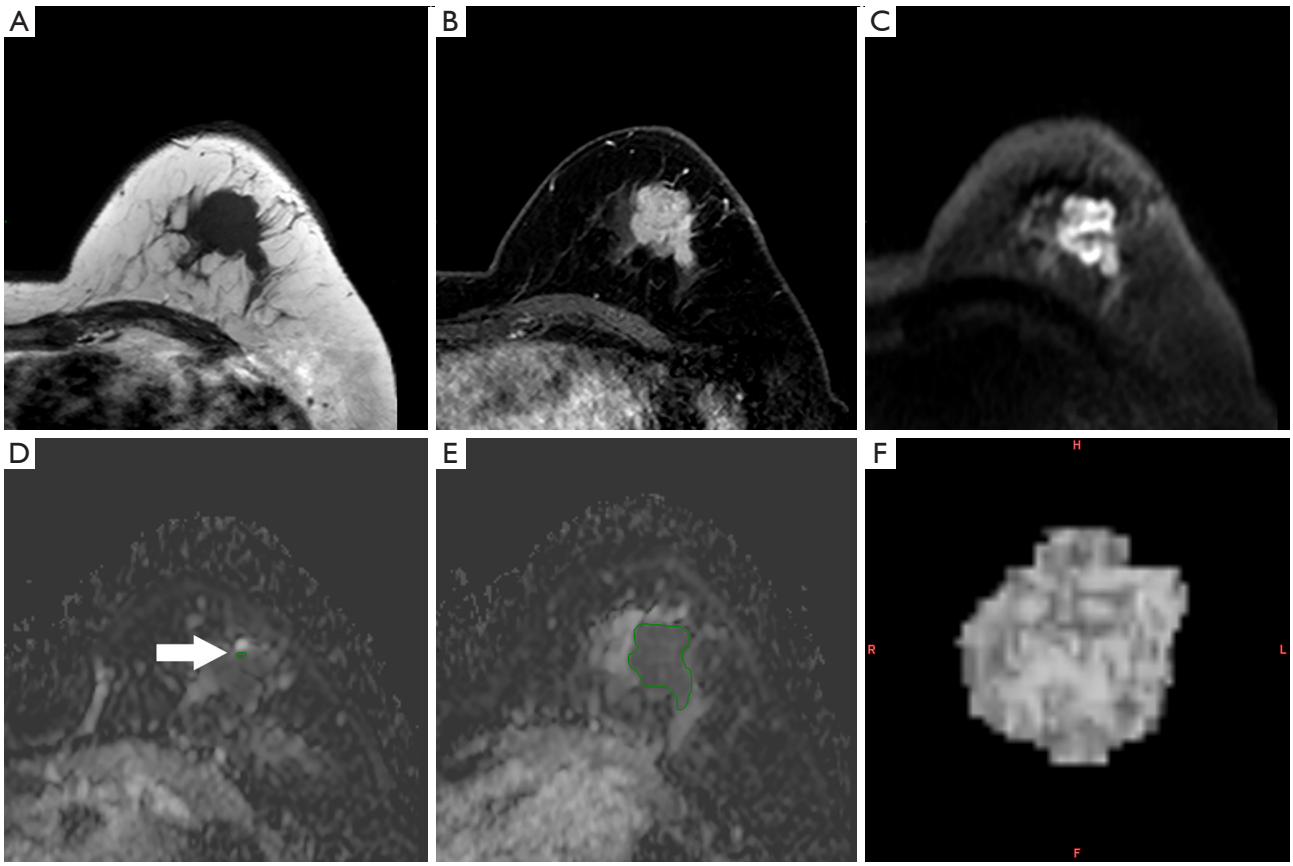

Figure 2 Images from a 49-year-old female patient with invasive ductal carcinoma confirmed by core needle biopsy in the left breast. (A) T1-weighted image. (B) Contrast-enhanced T1-weighted image. (C) DWI image with b=800 sec/mm^2. (D) Small 2D ROI (arrow). (E) Large 2D ROI were delimited on the ADC map. (F) Three-dimensional rendering of the volume ROI covering the whole lesion. DWI, diffusion weighted imaging; 2D, 2-dimensional; ROI, region of interest; ADC, apparent diffusion coefficient.

Table 1). There were 5 (7%) HER2-enriched tumors, 6 (8%) triple negative tumors, and 64 (85%) luminal type breast cancers including 30 (40%) luminal A and 34 (45%) luminal B. A significant difference in the distribution of luminal type, luminal A, and HER2-enriched tumors was noted between responders and non-responders (P=0.029£, 0.007, and P=0.027, respectively). There was no significant difference in the size of the ROI.

Inter- and intra-observer repeatability analysis

Inter- and intra-observer repeatability of the large 2D ROI and volume ROI methods were generally higher than those of the small 2D ROI method. In the case of inter- and intra-observer repeatability associated with the large 2D ROI and volume ROI methods, intra-observer repeatability were generally higher than inter-observer repeatability, and some parameters (mean, 10%, 25%, median in large 2D ROI and mean, 10%, 25%, median, 75% in volume ROI) of the ICCs were excellent (0.820–0.934). The results are summarized in *Table 2*.

A comparison of the ADC values among the three ROI methods

The ADC values of all patients were significantly different among the three ROI methods, with P<0.001 for all variables except for skewness (P=0.038) and the 10% percentile (P=0.006) (*Table 3*). The volume ROIs had the lowest minimum ($0.17\pm0.17\times10^{-3}$ mm^2/s; P<0.001 compared with the minimum values of other ROI methods) and the largest maximum ($2.33\pm0.55\times10^{-3}$ mm^2/s; P<0.001) ADC values.

Table 2 Inter- and intra-observer repeatability for the three ROI methods

Metrics	Inter-observer ICC	Intra-observer ICC
Small 2D ROI		
Mean	0.661	0.603
SD	0.091	0.207
Skewness	0.174	0.266
Kurtosis	0.281	0.084
Min	0.641	0.607
10%	0.631	0.603
25%	0.641	0.611
Median	0.639	0.598
75%	0.594	0.564
90%	0.566	0.431
Max	0.539	0.355
Large 2D ROI		
Mean	0.820	0.925
SD	0.492	0.772
Skewness	0.445	0.554
Kurtosis	0.236	0.366
Min	0.486	0.666
10%	0.845	0.881
25%	0.86	0.912
Median	0.821	0.934
75%	0.766	0.921
90%	0.685	0.88
Max	0.519	0.788
Volume ROI		
Mean	0.846	0.906
SD	0.765	0.793
Skewness	0.441	0.662
Kurtosis	0.545	0.761
Min	0.598	0.505
10%	0.924	0.875
25%	0.910	0.913
Median	0.832	0.905
75%	0.787	0.883
90%	0.764	0.867
Max	0.753	0.744

All units of the parameters are $\times 10^{-3}$ mm^2/s except for skewness and kurtosis. ROI, region of interest; ICC, intraclass correlation coefficient; 2D, 2-dimensional; SD, standard deviation; ROI, region of interest.

A comparison of the ADC values between responders and non-responders

Concerning the small 2D ROI method aspect, the mean, 10%, 25%, median, 75%, and 90% ADC values were all significantly higher in responders compared to non-responders ($P \leq 0.049$). In the large 2D ROI method, the minimum, 10%, 25%, and median ADC values were higher in responders compared to non-responders ($P \leq 0.033$). The same results were observed in the volume ROI minimum, 10%, 25%, and median ADC values ($P \leq 0.041$). Furthermore, the 10%, 25%, and median ADC values of the responders were significantly higher than those of non-responders in all 3 ROI methods (*Table 4*).

The ROC curves were generated to evaluate the diagnostic performances of the 3 ROI methods in predicting patient response (*Figure 3*). All areas under the curve (AUCs) for the 3 ROI methods ranged from 0.470 (maximum of the large 2D ROIs) to 0.701 (10% of the large 2D ROIs) (*Table 4*). When a 10% ADC cutoff value of 0.75×10^{-3} mm^2/s was used in the large 2D ROI method, the following diagnostic predictive values were acquired: sensitivity of 80.8%; specificity of 57.1%; positive predictive value (PPV) of 50.0%; negative predictive value (NPV) of 84.9%; and accuracy of 65.3%. The 10% area under the curve in large 2D ROIs was considered superior, however it was not significantly higher than 25% in the large 2D ROI method (AUC 0.688; P=0.589) and 10% in the volume ROI method (AUC 0.686; P=0.651).

A comparison of the histogram parameters between responders and non-responders according to molecular subtype

The histogram analysis results predicting response in different molecular subtype are displayed in *Table 5* and *Figure 4*. Some histogram ADC values were significantly higher in responders with luminal A tumors using the 3

Table 3 A comparison of ADC histogram values of the three ROI methods in all patients

Metrics	Small 2D ROI	Large 2D ROI	Volume ROI	P
Mean	0.82±0.25	1.09±0.24	1.10±0.22	<0.001*
SD	0.12±0.06	0.25±0.11	0.29±0.09	<0.001*
Skewness	0.25±0.68	0.23±0.55	0.45±0.50	0.038*
Kurtosis	2.85±1.10	3.75±1.39	4.30±1.68	<0.001*
Min	0.62±0.27	0.41±0.33	0.17±0.17	<0.001*
10%	0.67±0.27	0.80±0.23	0.76±0.21	0.006*
25%	0.73±0.26	0.93±0.23	0.91±0.21	<0.001*
Median	0.82±0.25	1.08±0.24	1.08±0.22	<0.001*
75%	0.89±0.25	1.24±0.26	1.27±0.25	<0.001*
90%	0.99±0.25	1.41±0.32	1.48±0.29	<0.001*
Max	1.07±0.29	1.90±0.60	2.33±0.55	<0.001*

All units of the parameters are $\times 10^{-3}$ mm^2/s except for skewness and kurtosis. *, indicates statistical significance (P<0.05). ADC, apparent diffusion coefficient; ROI, region of interest; 2D, 2-dimensional; SD, standard deviation.

Table 4 A comparison of ADC histogram values between responders and non-responders

Metrics	Responders (n=26)*	Non-responders (n=49)*	P	Sensitivity (%)	Specificity (%)	Cutoff value*	AUC
Small 2D ROI							
Mean	0.92±0.21	0.79±0.25	0.024#	88.46	40.82	0.710	0.634
SD	0.12±0.06	0.12±0.06	0.826	61.54	48.98	0.113	0.495
Skewness	0.22±0.62	0.27±0.71	0.752	69.23	44.90	0.115	0.502
Kurtosis	2.96±0.87	2.80±1.19	0.568	53.85	67.35	2.808	0.584
Min	0.72±0.24	0.59±0.27	0.063	84.62	34.69	0.515	0.594
10%	0.77±0.23	0.64±0.28	0.044#	84.62	36.73	0.562	0.594
25%	0.84±0.22	0.70±0.27	0.021#	92.31	36.73	0.593	0.619
Median	0.92±0.21	0.78±0.25	0.020#	88.46	42.86	0.698	0.644
75%	0.99±0.22	0.86±0.25	0.029#	84.62	42.86	0.794	0.638
90%	1.08±0.23	0.96±0.26	0.049#	50.00	73.47	1.048	0.643
Max	1.18±0.28	1.04±0.30	0.056	88.46	34.69	0.911	0.624
Large 2D ROI							
Mean	1.17±0.25	1.06±0.23	0.054	69.23	61.22	1.067	0.647
SD	0.21±0.08	0.27±0.12	0.062	84.62	44.90	0.255	0.619
Skewness	0.17±0.59	0.26±0.53	0.521	88.46	28.57	0.621	0.558
Kurtosis	3.79±1.76	3.71±1.18	0.810	26.92	85.71	2.719	0.517
Min	0.54±0.34	0.34±0.30	0.010#	50.00	79.59	0.620	0.658
10%	0.90±0.23	0.74±0.22	0.004#	80.77	57.14	0.750	0.701

Table 4 (*continued*)

Table 4 (*continued*)

Metrics	Responders (n=26)*	Non-responders (n=49)*	P	Sensitivity (%)	Specificity (%)	Cutoff value*	AUC
25%	1.03±0.23	0.88±0.21	0.007#	76.92	55.10	0.887	0.688
Median	1.17±0.25	1.04±0.22	0.033#	57.69	75.51	1.128	0.645
75%	1.31±0.27	1.21±0.26	0.153	69.23	55.10	1.196	0.616
90%	1.44±0.31	1.41±0.33	0.704	80.77	36.73	1.248	0.548
Max	1.82±0.44	1.94±0.66	0.440	73.08	36.73	1.614	0.470
Volume ROI							
Mean	1.17±0.23	1.07±0.21	0.057	80.77	55.10	1.033	0.648
SD	0.27±0.07	0.31±0.10	0.113	46.15	75.51	0.247	0.577
Skewness	0.41±0.42	0.47±0.54	0.596	42.31	71.43	0.577	0.486
Kurtosis	4.00±1.23	4.44±1.85	0.288	46.15	71.43	3.445	0.562
Min	0.26±0.20	0.12±0.13	0.001#	50.00	87.76	0.264	0.681
10%	0.85±0.21	0.72±0.21	0.008#	84.62	57.14	0.712	0.686
25%	0.99±0.21	0.87±0.20	0.018#	69.23	65.31	0.935	0.666
Median	1.16±0.23	1.05±0.21	0.041#	76.92	53.06	1.023	0.650
75%	1.34±0.26	1.25±0.24	0.161	57.69	67.35	1.279	0.620
90%	1.52±0.29	1.46±0.29	0.416	69.23	51.02	1.396	0.586
Max	2.24±0.48	2.39±0.58	0.277	76.92	46.94	2.449	0.580

ROC curves were generated for all ADC measurements for each ROI method. Sensitivity, specificity, and AUC were calculated under the optimal cut-off value listed for each item, which was determined according to the nearest point to the upper left corner of the ROC curve diagram. #, indicates statistical significance (P<0.05). *, all units of the parameters are $\times 10^{-3}$ mm^2/s except for skewness and kurtosis. ADC, apparent diffusion coefficient; 2D, 2-dimensional; ROI, region of interest; SD, standard deviation; ROC, receiver operating characteristic; AUC, area under the curve.

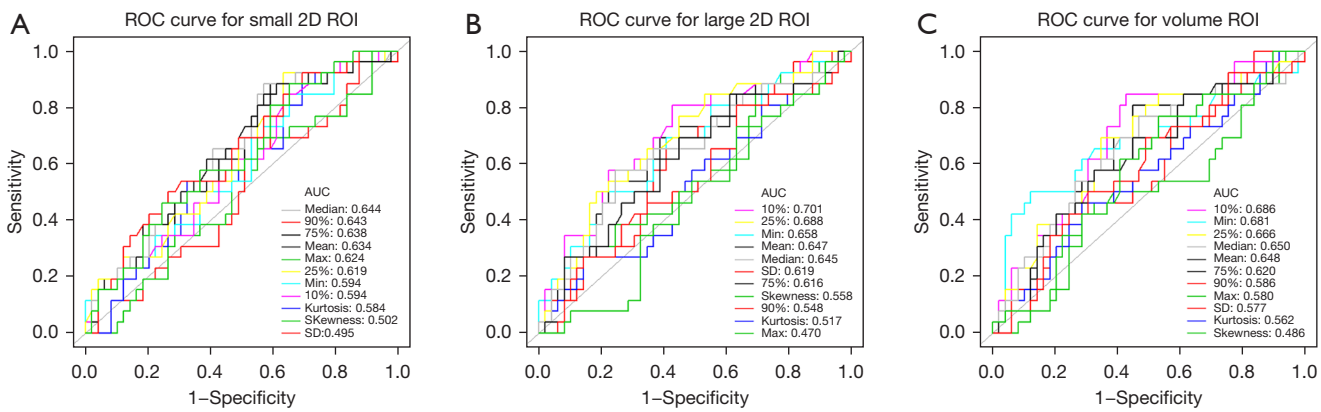

Figure 3 ROC curves calculated from 3 ROI methods using ADC histogram analysis for discriminating between responders and non-responders prior to neoadjuvant chemotherapy. (A) Small 2D ROI method. (B) Large 2D ROI method. (C) Volume ROI method. ROC, receiver operating characteristic; 2D, 2-dimensional; ROI, region of interest; ADC, apparent diffusion coefficient.

Table 5 A comparison of ADC histogram parameters between responders and non-responders according to molecular subtype

Metrics	Luminal A (n=30)				Luminal B (n=34)				Luminal type (n=64)			
	Responders (n=5)*	Non-responders (n=25)*	P	AUC	Responders (n=14)*	Non-responders (n=20)*	P	AUC	Responders (n=19)*	Non-responders (n=45)*	P	AUC
Small 2D ROI												
Mean	0.93±0.30	0.70±0.24	0.064	0.736	0.88±0.24	0.85±0.23	0.725	0.507	0.89±0.25	0.77±0.24	0.063	0.626
SD	0.16±0.10	0.12±0.07	0.359	0.632	0.10±0.05	0.12±0.05	0.423	0.593	0.12±0.07	0.12±0.06	0.878	0.528
Skewness	0.13±0.46	0.16±0.55	0.911	0.528	0.28±0.72	0.47±0.85	0.513	0.554	0.24±0.66	0.30±0.71	0.778	0.488
Kurtosis	2.52±0.72	2.35±0.77	0.644	0.416	3.23±0.95	3.35±1.51	0.787	0.532	3.04±0.94	2.80±1.25	0.439	0.619
Min	0.65±0.34	0.50±0.29	0.309	0.640	0.69±0.27	0.65±0.24	0.641	0.486	0.68±0.28	0.57±0.27	0.137	0.602
10%	0.72±0.32	0.54±0.29	0.220	0.664	0.75±0.26	0.71±0.23	0.671	0.518	0.74±0.27	0.61±0.27	0.099	0.611
25%	0.83±0.33	0.60±0.27	0.104	0.720	0.80±0.26	0.77±0.23	0.699	0.529	0.81±0.27	0.67±0.27	0.069	0.633
Median	0.92±0.32	0.70±0.24	0.077	0.712	0.87±0.24	0.83±0.23	0.599	0.539	0.89±0.25	0.76±0.24	0.057	0.638
75%	1.02±0.31	0.78±0.23	0.055	0.728	0.93±0.24	0.91±0.24	0.824	0.523	0.95±0.25	0.84±0.24	0.090	0.622
90%	1.14±0.31	0.87±0.23	0.028#	0.800	1.02±0.23	1.02±0.23	0.952	0.493	1.05±0.25	0.94±0.24	0.079	0.627
Max	1.29±0.43	0.94±0.27	0.022#	0.760	1.10±0.27	1.12±0.28	0.851	0.525	1.15±0.31	1.02±0.29	0.103	0.609
Large 2D ROI												
Mean	1.14±0.29	0.99±0.23	0.211	0.684	1.12±0.26	1.14±0.21	0.845	0.504	1.13±0.26	1.05±0.23	0.270	0.601
SD	0.18±0.05	0.29±0.15	0.126	0.776	0.21±0.09	0.25±0.08	0.225	0.652	0.2±0.08	0.27±0.12	0.035#	0.689
Skewness	0.12±0.49	0.25±0.48	0.613	0.584	0.30±0.65	0.29±0.63	0.952	0.491	0.25±0.61	0.26±0.54	0.948	0.488
Kurtosis	3.68±0.77	3.64±0.86	0.921	0.528	4.17±2.18	3.86±1.54	0.627	0.536	4.04±1.9	3.74±1.20	0.444	0.528
Min	0.62±0.42	0.22±0.23	0.005#	0.800	0.50±0.34	0.45±0.33	0.728	0.455	0.53±0.36	0.33±0.30	0.022#	0.677
10%	0.91±0.30	0.64±0.20	0.014#	0.804	0.87±0.23	0.85±0.21	0.747	0.541	0.88±0.24	0.73±0.23	0.019#	0.682
25%	1.02±0.29	0.80±0.20	0.044#	0.744	0.99±0.23	0.97±0.20	0.853	0.525	0.99±0.24	0.87±0.22	0.053	0.654
Median	1.14±0.30	0.97±0.23	0.165	0.704	1.11±0.25	1.13±0.21	0.830	0.491	1.12±0.26	1.04±0.23	0.239	0.604
75%	1.25±0.30	1.15±0.28	0.481	0.648	1.26±0.28	1.29±0.23	0.693	0.527	1.25±0.28	1.21±0.26	0.580	0.565
90%	1.35±0.29	1.36±0.37	0.954	0.512	1.39±0.34	1.47±0.27	0.473	0.561	1.38±0.32	1.41±0.33	0.759	0.511
Max	1.71±0.29	2.00±0.85	0.464	0.436	1.82±0.51	1.92±0.39	0.518	0.586	1.79±0.46	1.96±0.68	0.315	0.436

Table 5 (*continued*)

Table 5 (*continued*)

Metrics	Luminal A (n=30)				Luminal B (n=34)				Luminal type (n=64)			
	Responders (n=5)*	Non-responders (n=25)*	P	AUC	Responders (n=14)*	Non-responders (n=20)*	P	AUC	Responders (n=19)*	Non-responders (n=45)*	P	AUC
Volume ROI												
Mean	1.13±0.22	1.03±0.21	0.338	0.636	1.13±0.25	1.12±0.19	0.897	0.543	1.13±0.24	1.07±0.21	0.310	0.598
SD	0.28±0.07	0.32±0.13	0.567	0.472	0.26±0.08	0.30±0.06	0.172	0.621	0.27±0.08	0.31±0.10	0.133	0.406
Skewness	0.40±0.37	0.40±0.34	0.991	0.508	0.45±0.48	0.55±0.72	0.654	0.534	0.44±0.45	0.47±0.54	0.825	0.521
Kurtosis	3.94±1.21	4.22±1.47	0.698	0.560	4.18±1.38	4.92±2.36	0.305	0.589	4.12±1.31	4.53±1.92	0.401	0.556
Min	0.29±0.21	0.08±0.07	<0.001#	0.784	0.21±0.19	0.15±0.14	0.266	0.598	0.23±0.19	0.11±0.11	0.003	0.671
10%	0.79±0.13	0.65±0.18	0.118	0.736	0.82±0.22	0.78±0.23	0.646	0.546	0.81±0.20	0.71±0.21	0.084	0.642
25%	0.94±0.18	0.82±0.18	0.172	0.692	0.95±0.23	0.93±0.21	0.727	0.552	0.95±0.21	0.87±0.20	0.137	0.623
Median	1.11±0.25	1.00±0.21	0.298	0.632	1.11±0.25	1.09±0.19	0.825	0.546	1.11±0.24	1.04±0.21	0.251	0.598
75%	1.29±0.28	1.21±0.27	0.556	0.604	1.28±0.27	1.29±0.20	0.961	0.521	1.28±0.27	1.25±0.24	0.573	0.561
90%	1.49±0.26	1.43±0.34	0.731	0.596	1.46±0.31	1.49±0.21	0.733	0.511	1.47±0.29	1.46±0.29	0.904	0.537
Max	2.33±0.60	2.39±0.76	0.863	0.520	2.16±0.52	2.43±0.27	0.060	0.691	2.21±0.53	2.41±0.59	0.203	0.605

#, indicates statistical significance (P<0.05); *, all units of the parameters are $\times 10^{-3}$ mm^2/s except for skewness and kurtosis. ADC, apparent diffusion coefficient; 2D, 2-dimensional; ROI, region of interest; SD, standard deviation; AUC, area under the curve.

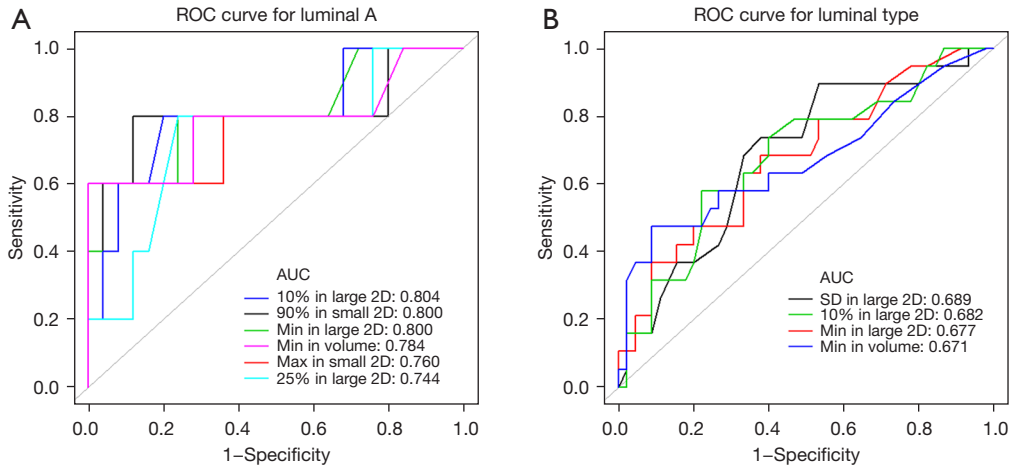

Figure 4 ROC curve to assess the differentiation between responders and non-responders prior to neoadjuvant chemotherapy in different subtypes. (A) 90%, max of small 2D ROI method, min, 10%, 25% of large 2D ROI method, min of volume ROI method in luminal A. (B) SD, min, 10% of large 2D ROI method, min of volume ROI method in luminal type. ROC, receiver operating characteristic; AUC, area under the curve; 2D, 2-dimensional; ROI, region of interest; SD, standard deviation.

ROI methods, and responders with luminal type tumors using the large 2D and volume ROI methods, except for SD in the large 2D ROI method for luminal type patients. For luminal A breast cancer, the histogram parameters of the 3 ROI methods, with significant differences between responders and non-responders, had similar AUCs ranging from 0.744 to 0.804. In luminal A type, 10% of large 2D ROI method showed the highest AUCs (0.804), with the following diagnostic predictive values: sensitivity of 80.0%; specificity of 80.0%; PPV of 44.5%; NPV of 95.2%; cut-off value of 0.760×10^{-3} mm^2/s; and accuracy of 80.0%. In luminal type, the SD of the large 2D ROI method had the highest AUC (0.689), with the following diagnostic predictive values: sensitivity of 89.5%; specificity of 46.7%; PPV of 41.5%; NPV of 91.3%; cut-off value of 0.255×10^{-3} mm^2/s; and accuracy of 59.4%.

Measurement time

The average measurement time differed significantly among the 3 ROI methods (P<0.001) with the volume ROI method requiring significantly more time (80.36±42.95 s) than the small 2D ROI and the large 2D ROI methods (6.08±1.29 and 8.04±3.26 s, respectively; P<0.001).

Discussion

ADC histogram parameters may be useful in predicting the responsiveness of breast cancer patients to NAC prior to administration. This study compared the repeatability and diagnostic performance of different ROI placement methods, including the small 2D ROI, large 2D ROI, and volume ROI methods. The results demonstrated that the ADC histogram values varied with different ROI methods. The large 2D ROI and volume ROI methods had excellent intra- and inter-observer repeatability in some parameters. The performance of 10% in the large 2D ROI method was superior, even in luminal A subtype tumors. In addition, the volume ROI required an increased measurement time compared to the other two ROI methods.

A number of reports have compared ROIs for breast cancer NAC response prediction (16,22,28). However, they failed to discuss the inter- and intra-observer repeatability and the volume ROI method was not included (16,22,28). In agreement with our findings, Newitt *et al.* reported good to excellent inter- and intra-observer repeatability for volume ADC, however, only mean values were reported (29). To the best of our knowledge, this current retrospective study is the first to examine the repeatability of three ROI methods in predicting response in breast cancer patients prior to NAC. The results demonstrated that the ICC of the median ADC value in intra-observer repeatability while using the large 2D ROI method was the highest, which was also higher than that reported in the study by Bickel *et al.* (highest ICC was obtained for the mean in the intra-observer using the large 2D ROI, 0.8848) (21). However, the large 2D

ROI method in the latter study was different from the one presented in our study. Indeed, the authors delimited the whole lesion on one slice that had the lowest ADC values as assessed visually, which was more subjective than in our present study. Giannotti *et al.* confirmed that the ICCs in the intra-observer were higher than the inter-observer (30), and the ICCs using the large 2D ROI method were higher than those of the small 2D ROI method, in agreement with our results. However, Giannotti and colleagues did not mention the patient group pathology and only discussed the mean ADC value. For the small 2D ROI method, the ROI area could be very similar to the other regions of the lesion. It is difficult to reach a consensus for observers. Although having a statistical significance, the small 2D ROI method is not appropriate in predicting response, mainly due to its poor repeatability. Similarly, Arponen *et al.* reported that the ICCs of the large 2D ROI method (0.817 for intra-observer, 0.831 for inter-observer) were higher than those of the small 2D ROI method (0.707 for intra-observer, 0.589 for inter-observer) (31). In contrast, Nogueira and colleagues reported better inter-observer repeatability for the small 2D ROI method [ICC =0.98, confidence interval (CI): 0.986–0.997] (32). However, the latter investigation used fewer parameters than that used in the current study, such as the mean, median, minimum, maximum, and SD, and therefore, the heterogeneity of the breast cancer cannot be fully demonstrated.

Significant differences in the histogram ADC values were detected among the 3 ROI methods. The volume ROIs were delineated slice by slice, while large 2D ROIs and small 2D ROIs contained only one slice. Indeed, the lowest and the highest cellular density may not occur in one slice. This explains why our volume ROI method had the lowest minimum and highest maximum ADC value. In conclusion, it is likely that ADC-derived histogram values can be influenced by the ROI method applied.

ADC-derived histogram analysis might have the potential to predict patient response prior to NAC, especially in certain molecular subtypes of breast cancer. Most previous reports have suggested that the pretreatment ADC value cannot predict response to NAC in breast cancer patients (10,15,16,20,28,33,34). To our knowledge, only Kim *et al.*, Cho *et al.*, and Minarikova *et al.* have studied responses prior to administration of NAC using histogram analysis (14-16,20), and concluded that ADC values were not capable of predicting response. Our results are in contrast to the above mentioned studies. The disagreement may be related to the fact that we have included more histogram parameters than the previous studies (Kim *et al.*: mean, 25%, median, 75%, and skewness; Cho *et al.*: mean, SD, minimum, maximum, kurtosis, and skewness; and Minarikova *et al.*: mean, median, 15%, 25%, 75%, and 90%) (14-16,20). Our results, based on relatively lower parameters (10%, 25%, and median in both ROI methods), suggested that ADC-derived histogram values can discriminate responders from non-responders. The lower ADC parameters may represent the most malignant areas of breast cancer (26). Our outcomes showed that the largest AUC was acquired in 10% ADC value in the large 2D ROI, which was similar to Kim *et al.* (0.70 in 75% D) and higher than Minarikova *et al.* (0.673 in 25% ADC) (14,16). Moreover, the abovementioned authors did not include a further discussion on the influence of ROI methods.

Our findings confirmed that, in the luminal A subtype, the diagnostic performance improved in the large 2D ROI and volume ROI methods. In breast cancers, different molecular subtypes have different prognosis and biological features, which are significantly relevant in clinical practice (35). Thus, it is important to choose an optimal ROI method for predicting NAC response depending on the different molecular subtypes in breast cancer. Bufi *et al.* reported an AUC of 0.787 in luminal type breast cancer, which is lower than that observed in our study (36). However, this latter investigation only used the large 2D ROI method and the mean for ADC values. Other authors have also failed to find any significance between responders and non-responders in luminal A or luminal type tumors (7,37). In these latter studies, only the 2D ROI method was used and only the mean for the ADC values was calculated. The AUC was the highest in the 10% of the large 2D ROI method in luminal A tumors, which was also the highest in the large 2D ROI method when molecular subtypes were not separated. Thus, our results showed that 10% in the large 2D ROI method is optimal for the luminal A subgroup, as well as for the whole study population, and the prediction performance was further improved in the luminal A subgroup.

There were some limitations to this report. First, this was a retrospective study, which may have given rise to selection bias. And the study cohort was relatively small, thus the statistical power may be reduced. More detailed analysis according to subtypes such as HER2 enriched and triple negative could not be conducted. These initial results should be further confirmed with a larger sample size in the future. Second, the ROIs were measured manually rather than automatically. Third, ROIs were not compared during or after NAC, as some lesions had disappeared during

or after NAC, and this may result in a substantial bias. However, this study is the first to focus on measurement methods in the prediction of NAC response in breast cancer patients using histogram analysis (14-16,20,38).

Conclusions

In conclusion, histogram ADC values can be influenced by the three ROI methods. The small 2D ROI method is not recommended in predicting response prior to NAC in breast cancer patients due to its poor repeatability. The predicting performance of ADC prior to NAC in breast cancer varies in different molecular subtype. When choosing the ROI method and histogram parameters in predicting response in breast cancer patients prior to NAC, 10% of the large 2D ROI method is recommended, in particular in luminal A subtype tumors.

Acknowledgments

Funding: This study was supported by grants from the Clinical Research Plan of Shanghai Shenkang Development Center (Nos. SHDC2020CR2008A and SHDC12021103) and Shanghai Municipal Commission of Economy and Informatization (No. 2019-RGZN-01094).

Footnote

Reporting Checklist: The authors have completed the STARD reporting checklist. Available at https://atm.amegroups.com/article/view/10.21037/atm-22-1078/rc

Data Sharing Statement: Available at https://atm.amegroups.com/article/view/10.21037/atm-22-1078/dss

Conflicts of Interest: All authors have completed the ICMJE uniform disclosure form (available at https://atm.amegroups.com/article/view/10.21037/atm-22-1078/coif). The authors have no conflicts of interest to declare.

Ethical Statement: The authors are accountable for all aspects of the work in ensuring that questions related to the accuracy or integrity of any part of the work are appropriately investigated and resolved. The study was conducted in accordance with the Declaration of Helsinki (as revised in 2013). The study was approved by institutional ethics board of Renji Hospital (No. KY2021-116-B). Informed consent was not required due to the retrospective nature of the study.

References

1. Untch M, Konecny GE, Paepke S, et al. Current and future role of neoadjuvant therapy for breast cancer. Breast 2014;23:526-37.
2. Hyder T, Bhattacharya S, Gade K, et al. Approaching Neoadjuvant Therapy in the Management of Early-Stage Breast Cancer. Breast Cancer 2021;13:199-211.
3. Fowler AM, Mankoff DA, Joe BN. Imaging Neoadjuvant Therapy Response in Breast Cancer. Radiology 2017;285:358-75.
4. Reig B, Lewin AA, Du L, et al. Breast MRI for Evaluation of Response to Neoadjuvant Therapy. Radiographics 2021;41:665-79.
5. Fangberget A, Nilsen LB, Hole KH, et al. Neoadjuvant chemotherapy in breast cancer-response evaluation and prediction of response to treatment using dynamic contrast-enhanced and diffusion-weighted MR imaging. Eur Radiol 2011;21:1188-99.
6. Park SH, Moon WK, Cho N, et al. Diffusion-weighted MR imaging: pretreatment prediction of response to neoadjuvant chemotherapy in patients with breast cancer. Radiology 2010;257:56-63.
7. Richard R, Thomassin I, Chapellier M, et al. Diffusion-weighted MRI in pretreatment prediction of response to neoadjuvant chemotherapy in patients with breast cancer. Eur Radiol 2013;23:2420-31.
8. Yuan L, Li JJ, Li CQ, et al. Diffusion-weighted MR imaging of locally advanced breast carcinoma: the optimal time window of predicting the early response to neoadjuvant chemotherapy. Cancer Imaging 2018;18:38.
9. Fujimoto H, Kazama T, Nagashima T, et al. Diffusion-weighted imaging reflects pathological therapeutic response and relapse in breast cancer. Breast Cancer 2014;21:724-31.
10. Bufi E, Belli P, Costantini M, et al. Role of the Apparent

Diffusion Coefficient in the Prediction of Response to Neoadjuvant Chemotherapy in Patients With Locally Advanced Breast Cancer. Clin Breast Cancer 2015;15:370-80.
11. Partridge SC, Zhang Z, Newitt DC, et al. Diffusion-weighted MRI Findings Predict Pathologic Response in Neoadjuvant Treatment of Breast Cancer: The ACRIN 6698 Multicenter Trial. Radiology 2018;289:618-27.
12. Hirano M, Satake H, Ishigaki S, et al. Diffusion-weighted imaging of breast masses: comparison of diagnostic performance using various apparent diffusion coefficient parameters. AJR Am J Roentgenol 2012;198:717-22.
13. Just N. Improving tumour heterogeneity MRI assessment with histograms. Br J Cancer 2014;111:2205-13.
14. Kim Y, Kim SH, Lee HW, et al. Intravoxel incoherent motion diffusion-weighted MRI for predicting response to neoadjuvant chemotherapy in breast cancer. Magn Reson Imaging 2018;48:27-33.
15. Cho GY, Gennaro L, Sutton EJ, et al. Intravoxel incoherent motion (IVIM) histogram biomarkers for prediction of neoadjuvant treatment response in breast cancer patients. Eur J Radiol Open 2017;4:101-7.
16. Minarikova L, Bogner W, Pinker K, et al. Investigating the prediction value of multiparametric magnetic resonance imaging at 3 T in response to neoadjuvant chemotherapy in breast cancer. Eur Radiol 2017;27:1901-11.
17. Kozumi M, Ota H, Yamamoto T, et al. Oesophageal squamous cell carcinoma: histogram-derived ADC parameters are not predictive of tumour response to chemoradiotherapy. Eur Radiol 2018;28:4296-305.
18. Wu LF, Rao SX, Xu PJ, et al. Pre-TACE kurtosis of ADCtotal derived from histogram analysis for diffusion-weighted imaging is the best independent predictor of prognosis in hepatocellular carcinoma. Eur Radiol 2019;29:213-23.
19. Bali MA, Pullini S, Metens T, et al. Assessment of response to chemotherapy in pancreatic ductal adenocarcinoma: Comparison between diffusion-weighted MR quantitative parameters and RECIST. Eur J Radiol 2018;104:49-57.
20. Kim YJ, Kim SH, Lee AW, et al. Histogram analysis of apparent diffusion coefficients after neoadjuvant chemotherapy in breast cancer. Jpn J Radiol 2016;34:657-66.
21. Bickel H, Pinker K, Polanec S, et al. Diffusion-weighted imaging of breast lesions: Region-of-interest placement and different ADC parameters influence apparent diffusion coefficient values. Eur Radiol 2017;27:1883-92.
22. Zhang D, Zhang Q, Suo S, et al. Apparent diffusion coefficient measurement in luminal breast cancer: will tumour shrinkage patterns affect its efficacy of evaluating the pathological response? Clin Radiol 2018;73:909.e7-909.e14.
23. Ogston KN, Miller ID, Payne S, et al. A new histological grading system to assess response of breast cancers to primary chemotherapy: prognostic significance and survival. Breast 2003;12:320-7.
24. Horvat JV, Iyer A, Morris EA, et al. Histogram Analysis and Visual Heterogeneity of Diffusion-Weighted Imaging with Apparent Diffusion Coefficient Mapping in the Prediction of Molecular Subtypes of Invasive Breast Cancers. Contrast Media Mol Imaging 2019;2019:2972189.
25. Horvat JV, Bernard-Davila B, Helbich TH, et al. Diffusion-weighted imaging (DWI) with apparent diffusion coefficient (ADC) mapping as a quantitative imaging biomarker for prediction of immunohistochemical receptor status, proliferation rate, and molecular subtypes of breast cancer. J Magn Reson Imaging 2019;50:836-46.
26. Suo S, Zhang K, Cao M, et al. Characterization of breast masses as benign or malignant at 3.0T MRI with whole-lesion histogram analysis of the apparent diffusion coefficient. J Magn Reson Imaging 2016;43:894-902.
27. DeLong ER, DeLong DM, Clarke-Pearson DL. Comparing the areas under two or more correlated receiver operating characteristic curves: a nonparametric approach. Biometrics 1988;44:837-45.
28. Belli P, Costantini M, Ierardi C, et al. Diffusion-weighted imaging in evaluating the response to neoadjuvant breast cancer treatment. Breast J 2011;17:610-9.
29. Newitt DC, Zhang Z, Gibbs JE, et al. Test-retest repeatability and reproducibility of ADC measures by breast DWI: Results from the ACRIN 6698 trial. J Magn Reson Imaging 2019;49:1617-28.
30. Giannotti E, Waugh S, Priba L, et al. Assessment and quantification of sources of variability in breast apparent diffusion coefficient (ADC) measurements at diffusion weighted imaging. Eur J Radiol 2015;84:1729-36.
31. Arponen O, Sudah M, Masarwah A, et al. Diffusion-Weighted Imaging in 3.0 Tesla Breast MRI: Diagnostic Performance and Tumor Characterization Using Small Subregions vs. Whole Tumor Regions of Interest. PLoS One 2015;10:e0138702.
32. Nogueira L, Brandão S, Matos E, et al. Region of interest demarcation for quantification of the apparent diffusion coefficient in breast lesions and its interobserver variability. Diagn Interv Radiol 2015;21:123-7.

33. Santamaría G, Bargalló X, Fernández PL, et al. Neoadjuvant Systemic Therapy in Breast Cancer: Association of Contrast-enhanced MR Imaging Findings, Diffusion-weighted Imaging Findings, and Tumor Subtype with Tumor Response. Radiology 2017;283:663-72.
34. Nilsen L, Fangberget A, Geier O, et al. Diffusion-weighted magnetic resonance imaging for pretreatment prediction and monitoring of treatment response of patients with locally advanced breast cancer undergoing neoadjuvant chemotherapy. Acta Oncol 2010;49:354-60.
35. Tang P, Tse GM. Immunohistochemical Surrogates for Molecular Classification of Breast Carcinoma: A 2015 Update. Arch Pathol Lab Med 2016;140:806-14.
36. Bufi E, Belli P, Di Matteo M, et al. Effect of breast cancer phenotype on diagnostic performance of MRI in the prediction to response to neoadjuvant treatment. Eur J Radiol 2014;83:1631-8.
37. Liu S, Ren R, Chen Z, et al. Diffusion-weighted imaging in assessing pathological response of tumor in breast cancer subtype to neoadjuvant chemotherapy. J Magn Reson Imaging 2015;42:779-87.
38. Chamming's F, Ueno Y, Ferré R, et al. Features from Computerized Texture Analysis of Breast Cancers at Pretreatment MR Imaging Are Associated with Response to Neoadjuvant Chemotherapy. Radiology 2018;286:412-20.

Cite this article as: Geng X, Zhang D, Suo S, Chen J, Cheng F, Zhang K, Zhang Q, Li L, Lu Y, Hua J, Zhuang Z. Using the apparent diffusion coefficient histogram analysis to predict response to neoadjuvant chemotherapy in patients with breast cancer: comparison among three region of interest selection methods. Ann Transl Med 2022;10(6):323. doi: 10.21037/atm-22-1078

